Downloaded from genesdev.cshlp.org on August 4, 2022 - Published by Cold Spring Harbor Laboratory Press

canoe encodes a novel protein containing a GLGF/DHR motif and functions with *Notch* and *scabrous* in common developmental pathways in *Drosophila*

Hiroshi Miyamoto,[1,3] Itsuko Nihonmatsu,[1] Shunzo Kondo,[1] Ryu Ueda,[1] Shin Togashi,[1] Kanako Hirata,[1] Yuko Ikegami,[1] and Daisuke Yamamoto[1,2,4]

[1]Mitsubishi Kasei Institute of Life Sciences, Machida, Tokyo 194, Japan;
[2]Yamamoto Behavior Genes Project, Exploratory Research for Advanced Technology (ERATO), Research Development Corporation of Japan (JRDC) at Mitsubishi Kasei Institute of Life Sciences, Machida-shi, Tokyo 194, Japan

The *canoe*^{misty1} (*cno*^{mis1}) mutation was isolated by virtue of its severe rough eye phenotype from ~500 fly lines, each harboring a single autosomal insertion of a P element (BmΔw). Excision of the P element generated a lethal, null allele, *cno*^{mis10}, together with many revertants with normal eye morphology. Ommatidia homozygous for *cno*^{mis10}, produced in an otherwise wild-type eye by somatic recombination, typically contain a reduced number of outer photoreceptors. Some *cno*^{mis1} homozygous adults bear extra macrochaetes on the head, notum, humerus and/or scutellum. *cno*^{mis1} hemizygotes often show conspicuous wing phenotypes such as a notched blade and the loss of a cross vein. The sequence of *cno* cDNA clones isolated from an embryonic cDNA library revealed a long open reading frame that potentially encodes a 1893-amino-acid protein with the GLGF/DHR motif, a conserved sequence in Discs large, Dishevelled, and some other proteins associated with cellular junctions. Flies doubly mutant for *cno*^{mis1} and *scabrous*^{1} (*sca*^{1}) and those for *cno*^{mis1} and the *split* (*spl*) allele of *Notch* (*N*) always have rumpled wings curved downward. The *spl; cno*^{mis1} double mutant flies also exhibit a "giant socket" phenotype. These phenotypes are rarely observed in flies singly mutant for either *cno*^{mis1}, *sca*^{1} or *spl*. The wing vein gaps caused by *Abruptex*^{1}, a *N* allele producing an activated form of N protein, are dominantly suppressed by *cno*^{mis1}. Heterozygosity for *shaggy* and *myospheroid* promotes formation of extra wing veins in *cno*^{mis1} homozygotes. The genetic interactions suggest that *cno* participates with members of the *N* pathway in regulating adhesive cell–cell interactions for the determination of cell fate.

[*Key Words*: *Drosophila; canoe*; GLGF/DHR motif; *Notch; scabrous*; cell–cell interactions; cellular patterning]

Received November 14, 1994; revised version accepted February 7, 1995.

The molecular mechanisms responsible for cellular pattern formation have been a major focus of developmental biology in the latest decade. *Drosophila melanogaster* proves to be the best suited organism for the study of cellular patterning, because of its relatively invariant pattern of cellular organization and amenability to genetics (Rubin 1988).

The *Notch* (*N*) gene has been studied intensively in *Drosophila* morphogenesis (Artavanis-Tsakonas et al. 1991; Campos-Ortega 1993). As inferred from its mutant phenotypes, *N* is a pleiotropic gene that functions in a variety of developmental processes: *N* activity is required for embryonic neurogenesis (Xu et al. 1990; Lieber et al. 1993) and for proper formation of the eyes (Fortini et al. 1993), wing (Rebay et al. 1993; de Celis and García-Bellido 1994), bristles (Heitzler and Simpson 1991), and egg chambers (Ruohola et al. 1991). The *N* gene product appears to play a permissive role, in the sense that it simply permits inductive cell–cell interactions by other, more specific mechanisms (Coyle-Thompson and Banerjee 1993). The *N* gene encodes a large transmembrane protein. The 1700-amino-acid extracellular domain contains a tandem array of 36 epidermal growth factor (EGF)-like repeats, and the 988-amino-acid cytoplasmic domain contains six copies of the ankyrin repeat (Wharton et al. 1985; Kidd et al. 1986). Genetic searches for mutations interacting with *N* identify N group genes, *Delta* (*Dl*), *Serrate* (*Ser*), *Enhancer of split* [*E(spl)*], *mastermind* (*mam*), *strawberry notch* (*sno*), and *deltex* (Coyle-Thompson and Banerjee 1993). *scabrous* (*sca*) (Baker et al. 1990) and *shaggy* (*sgg*)/*zeste-white 3* (*zw3*) (Perrimon and Smouse 1989) have also been implicated

[3]Present address: Faculty of Biology Oriented Science and Technology, Kinki University, Uchidacho, Naga-gun, Wakayama 649-64
[4]Corresponding author.

Downloaded from genesdev.cshlp.org on August 4, 2022 - Published by Cold Spring Harbor Laboratory Press

in the *N* pathway (Ruel et al. 1993). *Dl* and *Ser* are transmembrane proteins that have EGF-like repeats, with which they bind to specific sites of the N EGF-like repeats (Rebay et al. 1991). A recent experiment, using the two-hybrid system of yeast, indicates that Deltex, a cytoplasmic basic protein, directly associates with the N ankyrin repeat (Diederich et al. 1994). Apart from these examples, little is known about the mechanism of the signaling cascade. To understand thoroughly the developmental pleiotropy of the *N* function, identification of additional elements in the cascade and their molecular characterization are indispensable.

Toward this end, we have screened P-element insertion lines for the rough eye phenotype, and isolated a mutant, *misty* (*mis*), which displays a range of phenotypes similar to *N* in eye, bristle, and wing development. Furthermore, clear genetic interactions are demonstrated between *mis* and the mutations in the *N*-related genes, such as *sca*, *sgg*, and *N* itself. Molecular analysis revealed that *mis* encodes a novel cytoplasmic protein with a GLGF/DHR motif, defining a new class of possible downstream components of the *N* signaling pathway.

Results

Isolation and mapping of the mis *mutation*

We generated ~500 fly lines harboring single P-element insertions in the autosomes by means of the jump start mutagenesis (Cooley et al. 1988), in which a BmΔw element on the X chromosome was forced to translocate to an autosomal site by introducing the Δ2-3 P transposase source. Mutations were balanced with SM1 for second-chromosome insertions and with TM3 for third-chromosome insertions. The screening, which involves binocular examination of the compound eyes of homozygous adults from all lines except for those carrying lethal mutations, yielded the mis^1 mutation that exhibits a severe rough eye phenotype (Fig. 1b). The phenotype is linked with the P-element insertion, as its excision yields many revertant lines with normal eye morphology (Fig. 1a). A genomic DNA fragment flanking the BmΔw insertion in the mis^1 mutant was obtained by plasmid rescue and used as a probe for in situ hybridization to polytene chromosomes, revealing a single hybridizing signal at 82EF of the third chromosome (data not shown). To further define the locus cytologically, three deficiency chromosomes, *Df(3R)Z-1*, *Df(3R)3-4*, and *Df(3R)6-7*, bearing breakpoints in this region, were tested for allelism to mis^1. Only *Df(3R)6-7* produces the eye phenotype when placed in *trans* to the mis^1 mutation (Fig. 1c,g). *Df(3R)6-7* removes DNA in the cytological division 82D3-8 to 82F3-6 (S. Wasserman, pers. comm.). *Df(3R)Z-1* eliminates the cytological interval of 82A5,6–82E4, whereas *Df(3R)3-4* eliminates 82F1,2–82F10, 11. Therefore the *mis* mutation is located between 82E4, the right breakpoint of *Df(3R)Z-1*, and 82F1,2, the left breakpoint of *Df(3R)3-4*. In this cytological interval, an embryonic lethal mutation called *canoe* (*cno*) has been mapped (Jürgens et al. 1984). The transheterozygotes,

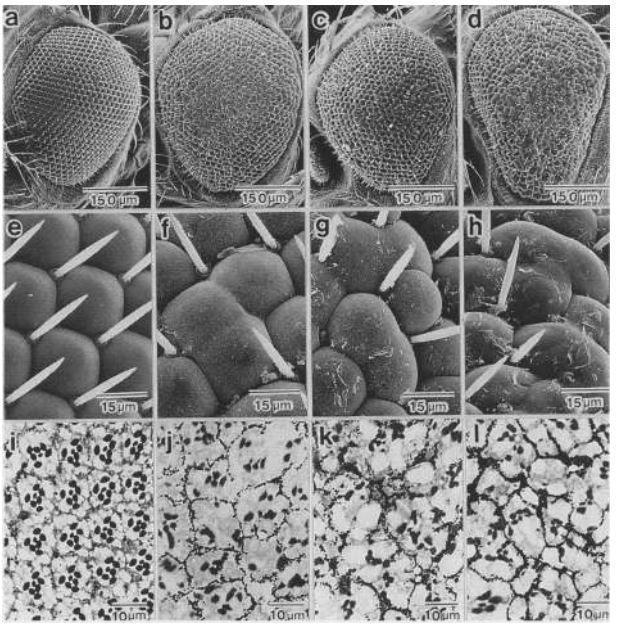

Figure 1. Adult eye phenotypes of the *mis* mutant flies. (*a*–h) SEM pictures of the eyes; (*i–l*) tangential eye sections of the same genotypes. (*a,e,i*) mis^{r13} (a revertant); (*b,f,j*) mis^1; (*c,g,k*) mis^1/ *Df(3R)6-7*; (*d,h,l*) mis^1/cno^{10BO1}.

mis^1/cno^{9K104} (data not shown) and mis^1/cno^{10B01} (Fig. 1d,h), had roughened eye structure, indicating that mis^1 is a new allele of the *cno* locus. mis^1 is thus referred to as cno^{mis1} hereafter.

Phenotypic characterization of cno^{mis1}

The wild-type *Drosophila* compound eye consists of ~800 identical subunits, called ommatidia. Each ommatidium contains 20 cells, including a central core of eight photoreceptors surrounded by pigment cells, which insulate them optically, and covered by a crystalline cone that directs light onto them (Basler and Hafen 1991; Ready 1989; Tomlinson 1988; Yamamoto 1993, 1994; Zipursky 1989).

The scanning electron microscopic (SEM) observations and the tangential sections of cno^{mis1} eyes reveal conspicuous features of the mutant ommatidia. The facets have irregular size and shape, and two or three adjacent ommatidia are often fused. The eye phenotypes are stronger in cno^{mis1}/cno^{10B01} and cno^{mis1}/*Df(3R)6-7* flies, where the number of photoreceptors contained in single ommatidia is decreased and the pigment cell lattice gets thicker than that of the wild type (Fig. 1k,l). The effect of the lethal excision allele, cno^{mis10}, on formation of the adult eye was examined by performing somatic mosaic analysis. cno^{mis10} may be a null allele, as no transcript can be detected in homozygous embryos by whole mount in situ hybridization (see Fig. 10I). Homozygous cno^{mis10} mutant cells were genetically marked using an ectopic copy of the *white*$^+$ (w^+) gene (a recessive gene affecting eye color), inserted in the third

Downloaded from genesdev.cshlp.org on August 4, 2022 - Published by Cold Spring Harbor Laboratory Press

chromosome near the *cno* locus, as a cell autonomous marker. Clones of homozygous mutant cells were made by inducing mitotic recombination with X-ray irradiation in the first larval instar. Photoreceptor cells that were w^- were homozygous mutant in an otherwise wild-type eye. When mutant patches of large size are formed, they are devoid of any ommatidia in some instances. Small mutant patches had ommatidia that were typically composed of a reduced number of photoreceptors. Because there is no lineage restriction in the formation of an ommatidium, cells of the different genotypes mix at the borders of mutant clones. Some such ommatidia had normal morphology, and others did not. Only cells in which cno^+ function is not required are expected to be cno^{mis10} in phenotypically normal ommatidia. It turned out that all of the photoreceptors could be cno^{mis10} without affecting the normal development of the ommatidium (Fig. 2). The simplest interpretation of the mosaic analysis is that the loss of *cno* function may be compensated by other gene products, as has been observed previously for some genes involved in sensory organ development. Another possibility is that *cno* is required outside of photoreceptor cell precursors. Because mutant cells were used to assemble normal ommatidia only in the small mutant patches or near the mosaic border, the surrounding wild-type cells might compensate the *cno* function lost from the mutant cells.

cno^{mis1} did not affect the initiation of ommatidium formation, as staining patterns revealed by mAb 22C10 and by the enhancer trap lines sca^{3853} and BB02, which serve as specific markers for R8, showed no obvious pattern defects in the larval eye disc (Fig. 3). However, cobalt sulfide staining of the pupal discs demonstrated that ommatidial assembly in this late stage is clearly distorted in cno^{mis1} homozygotes (Fig. 3). In cno^{mis1} eye discs, ommatidia having two, three, or five cone cells instead of four are occasionally found (Fig. 3). Ommatidia of mutant pupae often contain extra primary pigment cells (Fig. 3). Some of these ommatidia lack a secondary pigment cell, resulting in apparent fusion of adjacent facets (Fig. 3). These results suggest that the *cno* gene product is needed after pupation, as has been implied for the mutations in which the eye discs appear normal through the third instar but the adult eyes are irregular (Renfranz and Benzer 1989; Baker et al. 1992), although we cannot exclude the possibility that defects in the *cno* mutant eye could be the consequence of abnormalities present in the larval eye disc but too subtle to be detected in our light microscopic studies.

The mutant phenotype of cno^{mis1} is not restricted to

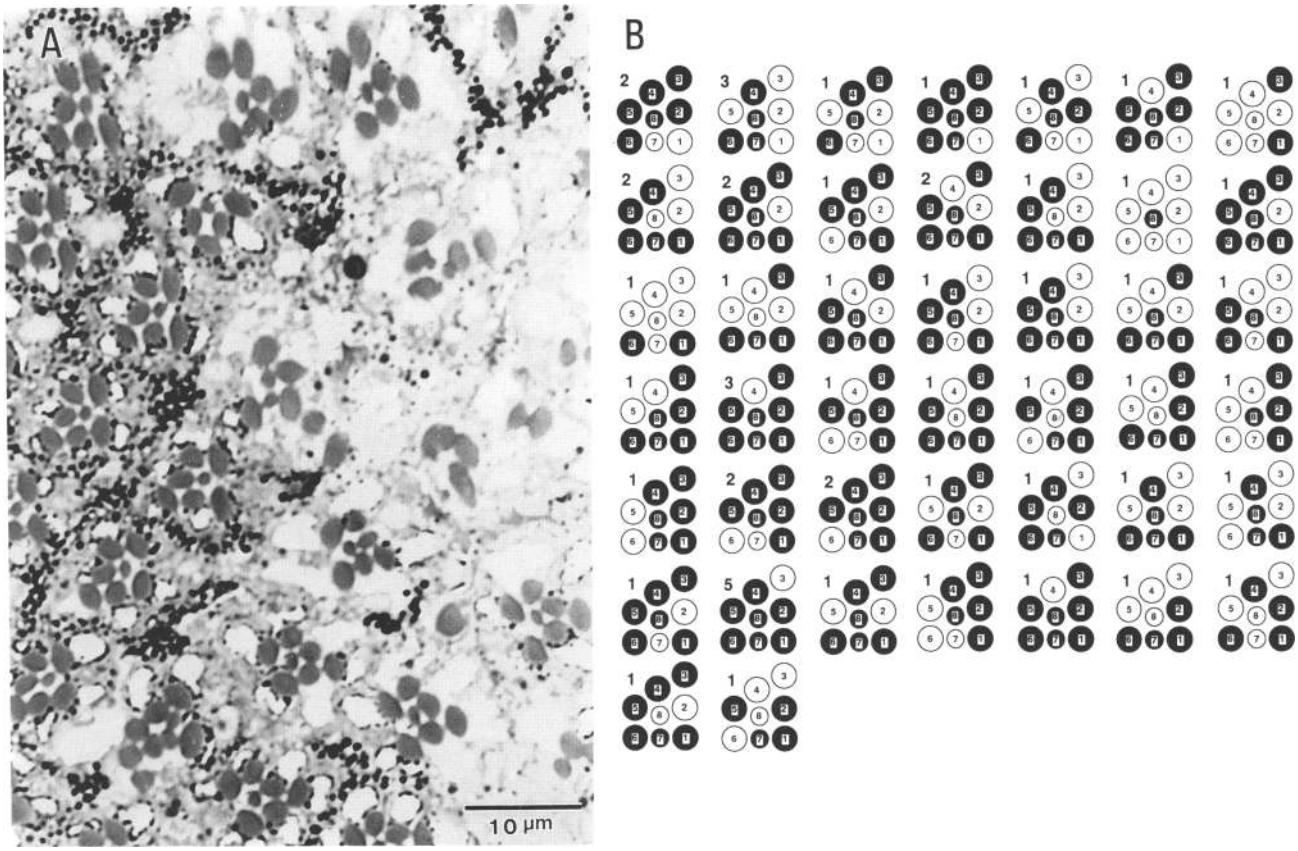

Figure 2. The compound eyes mosaic for the cno^{mis10} mutation. (*A*) An example of a large mutant clone. The genotypes of the photoreceptors R1–R8 in 58 normally developed mosaic ommatidia are shown schematically in B. (Solid circles) Wild-type cells; (open circles) mutant cells. The numerals indicate the number of cases for each pattern.

Downloaded from genesdev.cshlp.org on August 4, 2022 - Published by Cold Spring Harbor Laboratory Press

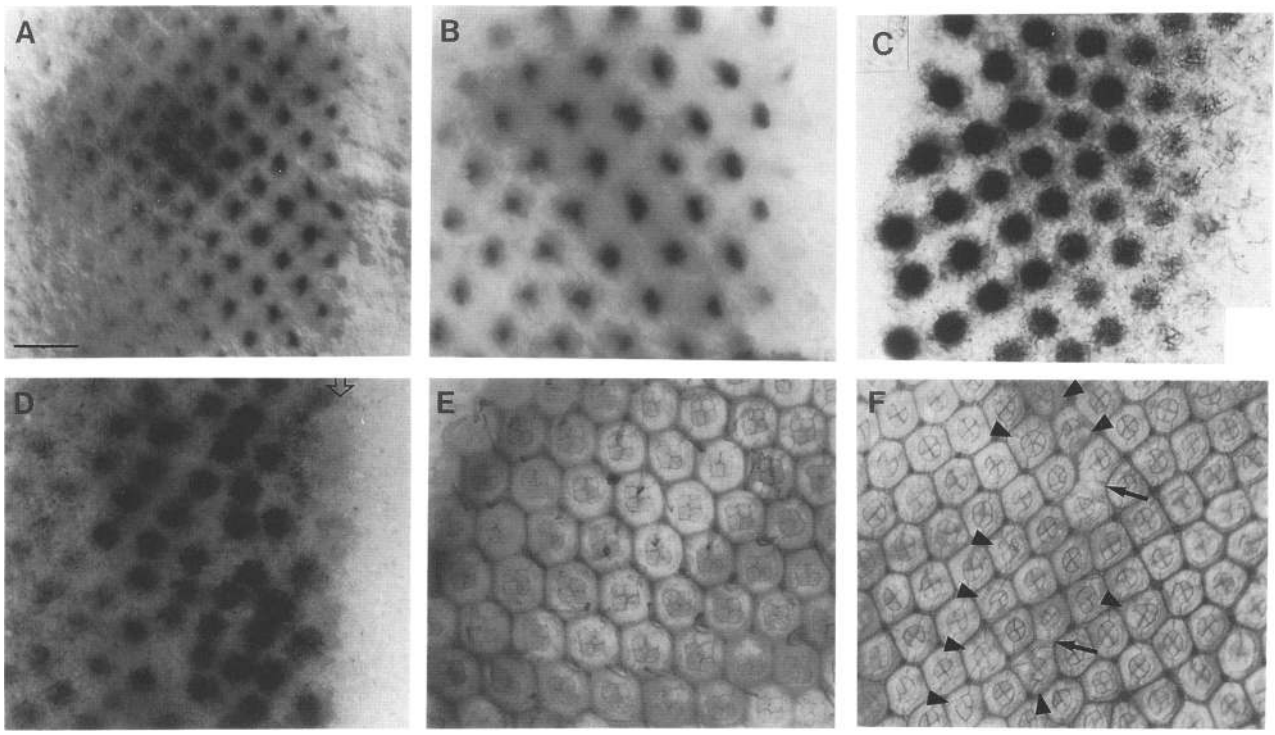

Figure 3. Phenotype analysis in the developing eye–antennal discs. (*A,B*) Larval discs of Canton-S wild-type (*A*) and cno^{mis1} (*B*) stained with mAb 22C10. (*C,D*) β-Galactosidase activity stainings of the cno^{mis1} discs from third instar larvae carrying a *lacZ* marker for R8, BB02 (*C*), and *sca* expression, sca^{3853} (*D*). β-Galactosidase expression in sca^{3853} eye discs starts in multiple cells near the anterior edge of the morphogenetic furrow (indicated by an open arrow) and becomes restricted to R8 precursor cells in the posterior columns. (*E,F*) Cobalt sulfide stainings of the pupal discs from Canton-S wild-type (*E*) and cno^{mis1} (*F*). In *F*, fused ommatidia are indicated by arrows. Examples of ommatidia containing too many or too few cone cells are indicated by arrowheads. Scale bar in (*A*), 39 μm for *A* and 30 μm for *B–F*. Anterior is to the *right*.

the eye. For example, extra macrochaetes (sensory bristles) are occasionally seen in the head, notum, and scutellum (Fig. 4). Although the structure of wings are normal for cno^{mis1} homozygotes, cno^{mis1} hemizygotes show variable but conspicuous wing phenotypes such as a notched blade and the loss of a cross vein (Fig. 6A–C).

Genetic interactions of cno *with the* N *group genes*

Fused ommatidia have been reported to occur in *sca* mutations (Baker et al. 1990). The *sca* mutants are also accompanied by bristle abnormalities (Mlodzik et al. 1990). The similarity in the phenotypes tempted us to examine possible genetic interactions between cno^{mis1} and sca^{1}. Although the compound eye of sca^{1} homozygotes contains some fused facets and others with excess or reduced number of photoreceptors, the majority of ommatidia have the normal complement of eight photoreceptors (Fig. 5a,f). When the sca^{1} homozygotes are also heterozygous for cno^{mis1}, the phenotype is dramatically enhanced so that many ommatidia are fused to each other (Fig. 5g). The eyes of the double homozygotes, sca^{1}; cno^{mis1}, are extremely rough, accompanied with giant ommatidia formed by fusions (Fig. 5c,d,h).

The bristle phenotype of sca^{1} was also enhanced by cno^{mis1} (Fig. 4). The enhancement is particularly clear in certain groups of macrochaetes, such as verticals, notopleurals, and dorsocentrals (Fig. 4). sca^{1}/sca^{1} individuals heterozygous or homozygous for cno^{mis1} bear more extra bristles than sca^{1}/sca^{1} does (Fig. 4). The synergistic interaction between sca^{1} and cno^{mis1} is most evident in the notoplurals: supernumerary bristles are frequently generated in sca^{1}/sca^{1}; $cno^{mis1}/+$ and sca^{1}/sca^{1}; cno^{mis1}/cno^{mis1}, whereas no extra bristle of this group is found in flies singly mutant for sca^{1} or cno^{mis1} (Fig. 4).

The genetic interaction between sca^{1} and cno^{mis1} is further revealed by examining wing morphology (Fig. 6E). Flies doubly mutant for cno^{mis1} and sca^{1} always have rumpled wings curved downward, with occasional shortening of the anterior cross vein. These phenotypes are not observed in flies singly mutant for either cno^{mis1} or sca^{1} (Fig. 6A,D).

Another mutation found to interact genetically with cno^{mis1} is the *split* (*spl*) allele of *N*. The *spl* mutation by itself causes severe roughness of the compound eye (Fig. 5i,j). The overall feature of the *spl*; cno^{mis1} eye is similar to that of *spl*, although the incidence of observing fused ommatidia is somewhat higher in the double mutant (Fig. 5k,l). The "nonadditive" nature of the *spl* and cno^{mis1} phenotypes is confirmed by examining the inter-

Downloaded from genesdev.cshlp.org on August 4, 2022 - Published by Cold Spring Harbor Laboratory Press

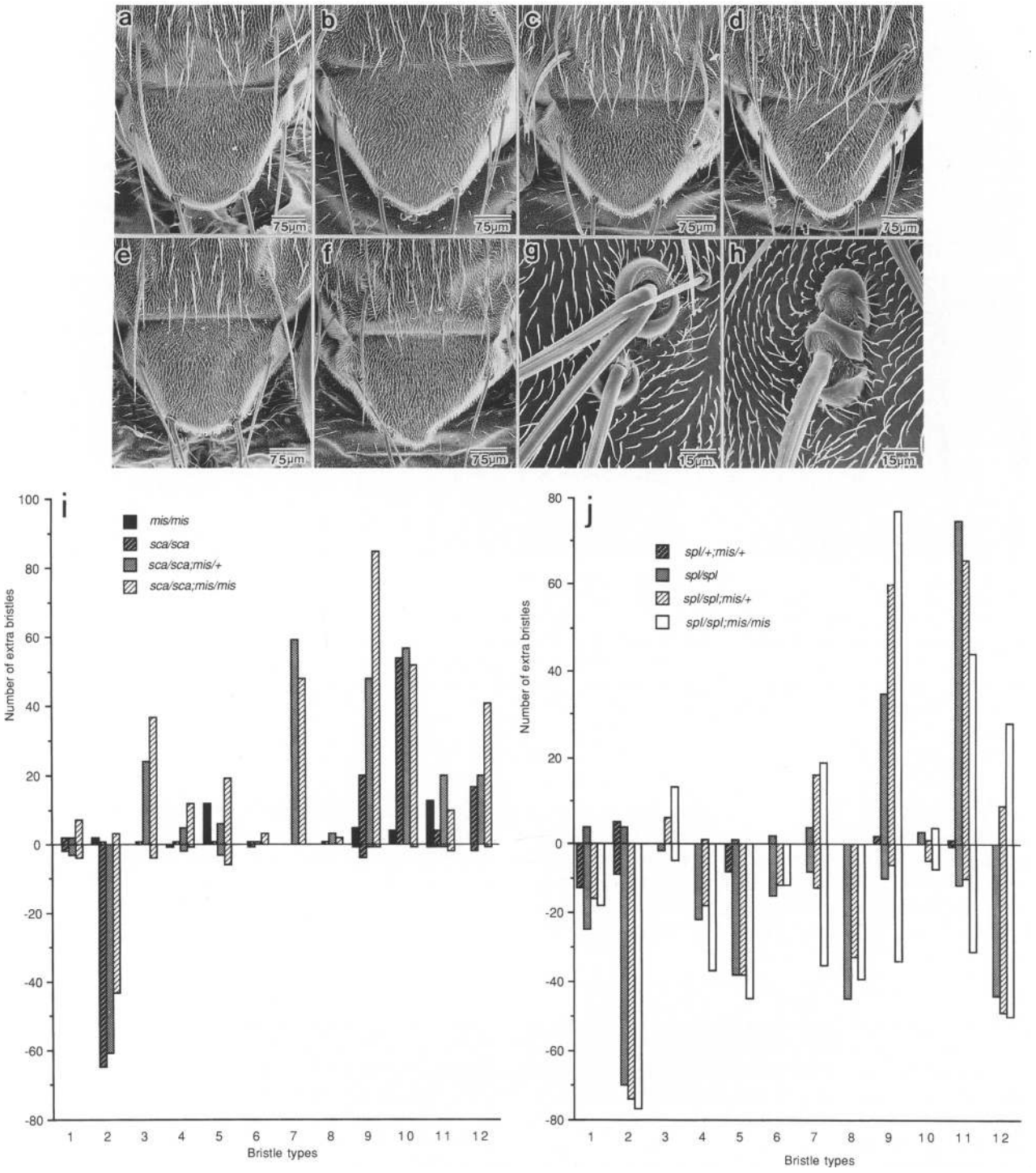

Figure 4. Genetic interactions of cno^{mis1} with sca^{1} and *spl* in the sensory bristles. The dorsal structures observed with SEM are shown for Canton-S wild-type (*a*), cno^{mis1} (*b*), sca^{1} (*c*), *spl* (*d*), sca^{1}; cno^{mis1} (*e*), and *spl*; cno^{mis1} (*f*). The giant sockets and duplicated bristles characteristic to the double mutants, sca^{1}; cno^{mis1} (*g*) and *spl*; cno^{mis1} (*h*) are shown at a higher magnification. (*i*,*j*) Quantification of genetic interactions between cno^{mis1} and sca^{1} (*i*) and cno^{mis1} and *spl* (*j*) in the sensory bristle phenotype. The number of extra bristles are counted for 40 specimens for each genotype, and the cumulative number is shown in the ordinate. The bristle types are indicated by the number in the abscissa: anterior, medial, and posterior orbitals (*1*), ocellar (*2*), anterior and posterior verticals (*3*), postvertical (*4*), upper and lower humerals (*5*), presutural (*6*), anterior and posterior notopleurals (*7*), anterior and posterior supra-alars (*8*), anterior and posterior dorsocentrals (*9*), anterior and posterior postalars (*10*), anterior and posterior scutellars (*11*), and anterior, medial, and postrior sternopleurals (*12*). The negative values in the ordinate indicates that the relevant bristles are lost (all bristles devoid of shafts are included regardless of the presence or absence of sockets).

Downloaded from genesdev.cshlp.org on August 4, 2022 - Published by Cold Spring Harbor Laboratory Press

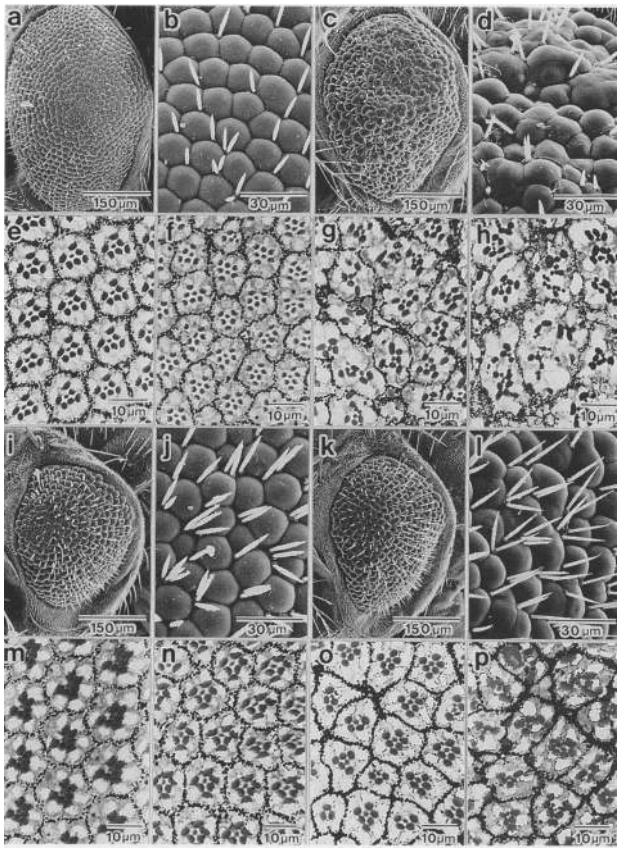

Figure 5. Genetic interactions of cno^{mis1} with sca^1 and *spl* in the compound eye. SEMs (*a–d*, *i–l*) and tangential sections (*e–h*, *m–p*) of sca^1 (*a,b,f*), $sca^1/+$ (*e*), sca^1; $cno^{mis1}/+$ (*g*), sca^1; cno^{mis1} (*c,d,h*), *spl* (*i,j,o*), *spl*/+ (*m*), *spl*/+; $cno^{mis1}/+$ (*n*), and *spl*; cno^{mis1} (*k,l,p*). cno^{mis1} dominantly enhances the sca^1 phenotype, whereas it has a moderate effect on *spl*. For wild type, see Fig. 1, *a*, *e*, and *i*.

nal structure of the ommatidia (Fig. 5m–p). The best example of this is seen in the double heterozygote *spl*/+; $cno^{mis1}/+$, in which ommatidia with too many or too few photoreceptors are found frequently in the compound eye (Fig. 5n). However, the phenotype of the double homozygote *spl*; cno^{mis1} is only slightly more severe than that of *spl* itself. It might be that the *spl* mutation was strong enough to block almost completely the *N* signaling in eye development, so that only a small effect was produced by the cno^{mis1} mutation.

In contrast to the situation found in the compound eye, cno^{mis1} dominantly enhances the *spl* bristle phenotype (Fig. 4d–h). The *spl* mutation may increase or decrease the number of bristles depending on the individuals or on the types of the bristles. The macrochaetes of the notopleural, dorsocentral, and scutellar groups are very sensitive to the cno^{mis1} dosage (Fig. 4). Reducing the dose of *cno* evidently potentiates *spl* in eliminating and overproducing macrochaetes, and the double mutant flies display phenotypes more severe than those expected from a simple arithmetic sum of the effects from *spl* and cno^{mis1} (Fig. 4). Remarkably, extremely large sockets with or without the bristle shafts are observed routinely in the double mutants, particularly in *spl*; cno^{mis1}, though such "giant" sockets are also found in flies singly mutant for *spl* or sca^1 at lower frequencies (Fig. 4g,h). The phenotype of the double mutants resembles that reported for the *Hairless* (*H*) mutant. In *H*, bristles are either lost (i.e., the shaft and socket fail to appear) or they exhibit a "double socket" phenotype, in which the shaft is apparently transformed into a second socket (Bang et al. 1991).

spl; cno^{mis1} has rumpled wings that are strikingly similar to those of sca^1; cno^{mis1}, although *spl* itself has no detectable effect on wing morphology (Fig. 6F,G). Complete loss of function of *N* leads to embryonic lethality and extreme hyperplasia of the nervous system. The phenotype shown by females hemizygous for the *N* locus is characterized by "notching" of the tips and/or edges of the wings (Fig. 6H). This dominant effect of the *N* deletion is enhanced in cno^{mis1} homozygotes. The wings of $N^{55e11}/+$; cno^{mis1} are rumpled, and the anterior cross veins are often shortened as they are in sca^1; cno^{mis1} and *spl*; cno^{mis1} (Fig. 6I). The *Abruptex* (*Ax*) alleles are dominant gain-of-function mutations, which typically produce wing vein gaps (Fig. 6J). The wing vein gaps caused by Ax^1 are partially restored in cno^{mis1} heterozygotes (Fig. 6K) and fully recovered in cno^{mis1} homozygotes (Fig. 6L).

We also found that mutations at two other loci, *sgg* and *myospheroid* (*mys*) interact with cno^{mis1} in wing morphogenesis. In cno^{mis1} homozygotes that are heterozygous for a null, lethal allele of *sgg* (sgg^{D127}), an extra vein develops above the middle portion of the second longitudinal vein (Fig. 7B), whereas $sgg^{D127}/+$ flies have normal wing structure when they are wild-type for the *cno* locus (data not shown). A similar extra vein is seen in cno^{mis1} homozygotes when they are heterozygous for a null, lethal allele of *mys* (mys^{XG43}) (Fig. 7D). In addition, these flies may have another extra vein, which arises from the posterior cross vein toward the second posterior cell. Again, no such phenotype can be detected in mys^{XG43} heterozygotes in the cno^+ genetic background (data not shown). mys^{nj42} is a hypomorphic mutation that yields viable homozygous adults with normal wings (Grinblat et al. 1994). mys^{nj42}; cno^{mis1} is practically lethal, with the few escapers having undersized wings (Fig. 7C). The wings of the double mutant may have a normal pattern of veins or be accompanied by an extra cross vein connecting the second and third longitudinal veins near the wing base (Fig. 7C). It has been reported that the mys^{XG43} mutant embryo has a profound dorsal hole (Leptin et al. 1989; Brown 1994), reminiscent of the embryo homozygous for *cno* (Jürgens et al. 1984).

Molecular characterization of the cno *gene*

We isolated a genomic DNA fragment adjacent to the P-element insertion site by plasmid rescue. The isolated fragment was then used to screen a phage library to recover genomic DNA flanking the rescued region. North-

Downloaded from genesdev.cshlp.org on August 4, 2022 - Published by Cold Spring Harbor Laboratory Press

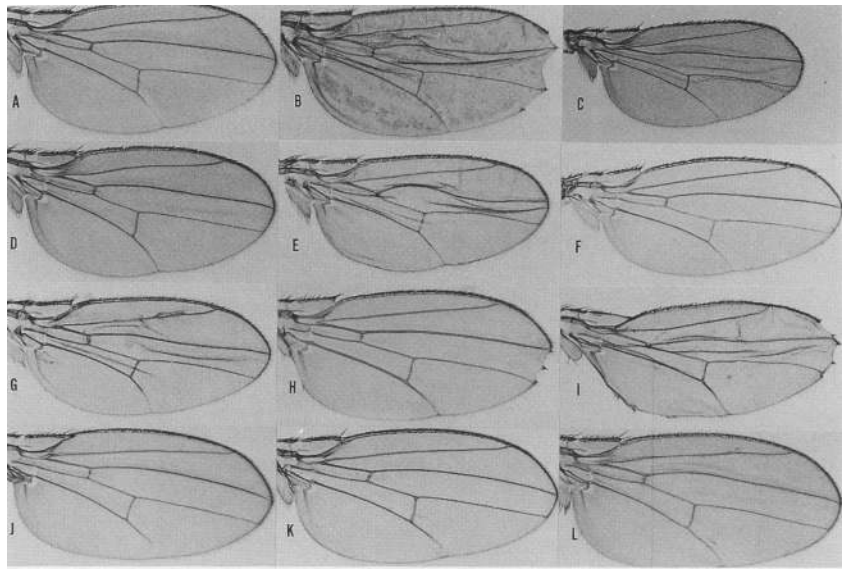

Figure 6. Genetic interactions of cno^{mis1} with sca^{1} and *N* alleles in wing morphology. Wings are shown for cno^{mis1} (*A*), $cno^{mis1}/Df(3R)6\text{-}7$ (*B,C*), sca^{1} (*D*), sca^{1}; cno^{mis1} (*E*), *spl* (*F*), *spl*; cno^{mis1} (*G*), $N^{55e11}/+$ (*H*), $N^{55e11}/+$; cno^{mis1} (*I*), $Ax^{1}/+$ (*J*), $Ax^{1}/+$; $cno^{mis1}/+$ (*K*), and $Ax^{1}/+$; cno^{mis1} (*L*). sca^{1} (*D*) and *spl* (*F*) wings are indistinguishable from those of wild-type.

ern blotting with poly(A)$^+$ mRNA from adults reveals that several transcription units are nested in the 15-kb genomic region cloned. Only one of these units is discernibly affected by the P-element insertion, making it a likely candidate for the *cno* gene (Fig. 8B). This transcription unit produces a triplet of mRNAs of 7.0, 7.5, and 8.2 kb in length, which are greatly reduced in their amount by the cno^{mis1} mutation. Precise excision of the P element restores all three transcripts, as exemplified in the revertant cno^{misr13} (Fig. 8B). A comparison of sequences of the genomic DNA from cno^{mis1} and a cDNA (see below) demonstrated that the P element is inserted 442 bp upstream of the tentative translation start site of the transcription unit. Based on these observations we identified this transcription unit as the *cno* gene. *cno* is a very large gene composed of 15 exons, spanning over 70 kb of the genome (Fig. 8A).

The wild-type *cno* mRNAs are most abundant in embryos (Fig. 8C). The transcripts decrease gradually toward the end of the larval stage and increase again in pupae and adults (Fig. 8C). The relative abundance of three transcripts changes depending on the developmental stages (Fig. 8C). Primer extention experiments with a cDNA (see below) suggest a single transcription start site that is located 612 bp upstream of the likely translation start (Fig. 8D). Because three possible adenylation signals are found in the 3′ end of a cDNA clone (Fig. 9a), it appears plausible that the different sizes of the transcripts reflect different polyadenylation sites.

The first cDNA clone was obtained by screening an eye disc cDNA library. Subsequently, screening of an embryonic cDNA library was repeated until the clones covered the full length of the transcripts. Sequence analysis (Fig. 9a) reveals that the *cno* cDNAs have a long open reading frame that potentially encodes a 1893-amino-acid protein with the GLGF/DHR motif (Cho et al. 1992; Woods and Bryant 1993). This sequence motif is conserved in *discs large*, [(*dlg*) Woods and Bryant 1991], *dishevelled* [(*dsh*) Klingensmith et al. 1994; Theisen et al. 1994], the mouse *dsh* homolog (*dvl*; Klingensmith et al. 1994), postsynaptic density protein 95 (Cho et al. 1992), nitric oxide synthase (NOS) (Bredt et al. 1991), tight junction-associated protein ZO-1 (Itoh et al. 1993), erythrocyte major palmitoylated protein p55 (Ruff et al. 1991), intracellular protein tyrosine phosphatase (PTP-meg; Gu et al. 1991), and the putative Friedriech ataxia gene product X11 (Duclos et al. 1993) (Fig. 9b).

The pattern of *cno* mRNA distribution was examined by digoxigenin in situ hybridization of whole-mount embryos (Fig. 10A–H). In early stage 5 embryos before cellularization, mRNA distributes uniformly at a low level throughout the embryos, except for the pole cells. At the cellular blastderm stage, signals are detected along the dorsal midline, where three intensely stained domains (anterior, central, and posterior) are discernible. In addition, three ectodermal stripes reminiscent of parasegmental expression of gap genes are seen clearly in the central domain of the embryo. In stages 7–10, expression

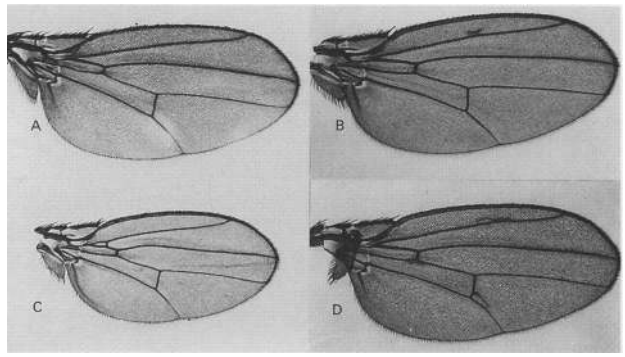

Figure 7. Genetic interactions of cno^{mis1} with sgg^{D127} and *mys* alleles. Wings of cno^{mis1} (*A*), $sgg^{D127}/+$; cno^{mis1} (*B*), mys^{nj42}; cno^{mis1} (*C*), and $mys^{XG43}/+$; cno^{mis1} (*D*) are shown.

Downloaded from genesdev.cshlp.org on August 4, 2022 - Published by Cold Spring Harbor Laboratory Press

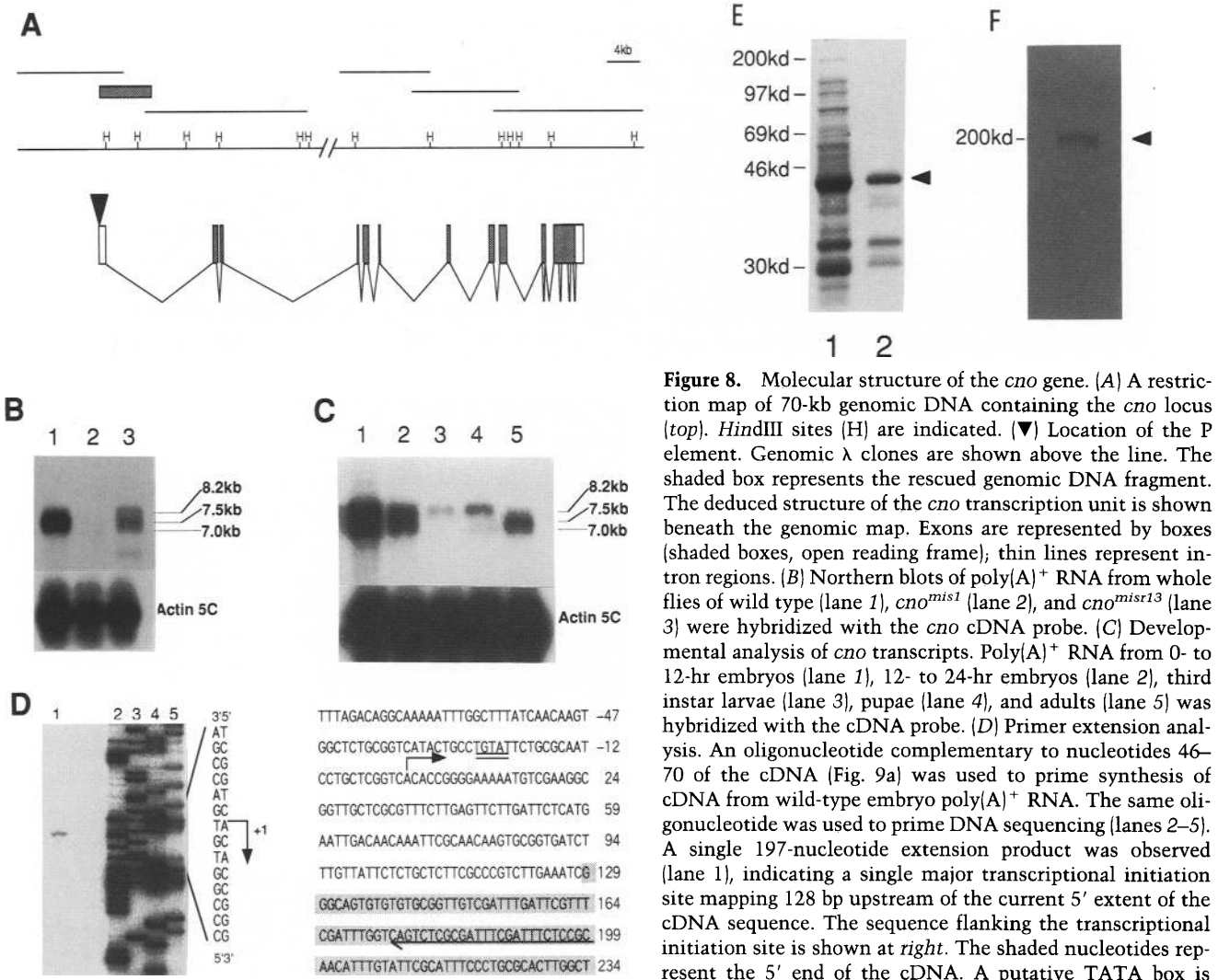

Figure 8. Molecular structure of the *cno* gene. (*A*) A restriction map of 70-kb genomic DNA containing the *cno* locus (*top*). *Hin*dIII sites (H) are indicated. (▼) Location of the P element. Genomic λ clones are shown above the line. The shaded box represents the rescued genomic DNA fragment. The deduced structure of the *cno* transcription unit is shown beneath the genomic map. Exons are represented by boxes (shaded boxes, open reading frame); thin lines represent intron regions. (*B*) Northern blots of poly(A)$^+$ RNA from whole flies of wild type (lane *1*), cno^{mis1} (lane *2*), and cno^{misr13} (lane *3*) were hybridized with the *cno* cDNA probe. (*C*) Developmental analysis of *cno* transcripts. Poly(A)$^+$ RNA from 0- to 12-hr embryos (lane *1*), 12- to 24-hr embryos (lane *2*), third instar larvae (lane *3*), pupae (lane *4*), and adults (lane *5*) was hybridized with the cDNA probe. (*D*) Primer extension analysis. An oligonucleotide complementary to nucleotides 46–70 of the cDNA (Fig. 9a) was used to prime synthesis of cDNA from wild-type embryo poly(A)$^+$ RNA. The same oligonucleotide was used to prime DNA sequencing (lanes *2–5*). A single 197-nucleotide extension product was observed (lane 1), indicating a single major transcriptional initiation site mapping 128 bp upstream of the current 5′ extent of the cDNA sequence. The sequence flanking the transcriptional initiation site is shown at *right*. The shaded nucleotides represent the 5′ end of the cDNA. A putative TATA box is indicated by a double underline. The arrow above the nucleotide sequence indicates the transcriptional initiation site. The oligonucleotides used for primer extension analysis are underlined. (*E,F*) Expression of the Cno protein. (*E*) Bacterial expression of a GST–Cno fusion protein. (Lane *1*) Total cell lysate from bacterial cells transformed with a plasmid expressing the GST–Cno fusion protein; (lane *2*) purified GST–Cno fusion protein. (*F*). Western blotting of protein extracts from wild-type embryos with Cno antiserum.

is confined to the dorsal furrows and the posterior midgut rudiment. The pattern of mRNA distribution may imply that Cno is required for delamination of presumptive endodermal cells, a process that depends on strict control of adhesion between midgut epithelial cells (Reuter et al. 1993; Tepass and Hartenstein 1994; see also Hartenstein et al. 1992 for a role of *N* in this process). Ectodermal expression becomes evident in stage 10. In stage 13, focal stainings are detected near the attachment site of the midgut with the foregut and hindgut. No staining is observed in approximately one-fourth of embryos from the cno^{mis10} balanced stock (Fig. 10I), indicating that the riboprobe detects specifically the *cno* transcripts.

A similar in situ hybridization experiment in eye–antennal discs shows that the *cno* transcripts are expressed ubiquitously, with a higher level of expression in the lateral edge region (Fig. 10J,K).

In an attempt to identify the Cno protein, we expressed a polypeptide corresponding to amino acids 122–258 of the Canoe protein as a fusion with glutathione *S*-transferase (GST) in *Escherichia coli* (Fig. 8E). The fusion protein that is effectively induced by isopropyl-β-D-thiogalactopyranoside (IPTG) was purified by chromatography on glutathione–agarose beads. Rabbits were injected with the bacterially expressed fusion protein for antiserum production. The immunized antiserum was then purified by affinity chromatography.

The antiserum recognizes a single band of ~200 kD in Western blotting of protein extracts from wild-type embryos (Fig. 8F). This result is consistent with the notion that the size difference of the transcripts is attributable

Downloaded from genesdev.cshlp.org on August 4, 2022 - Published by Cold Spring Harbor Laboratory Press

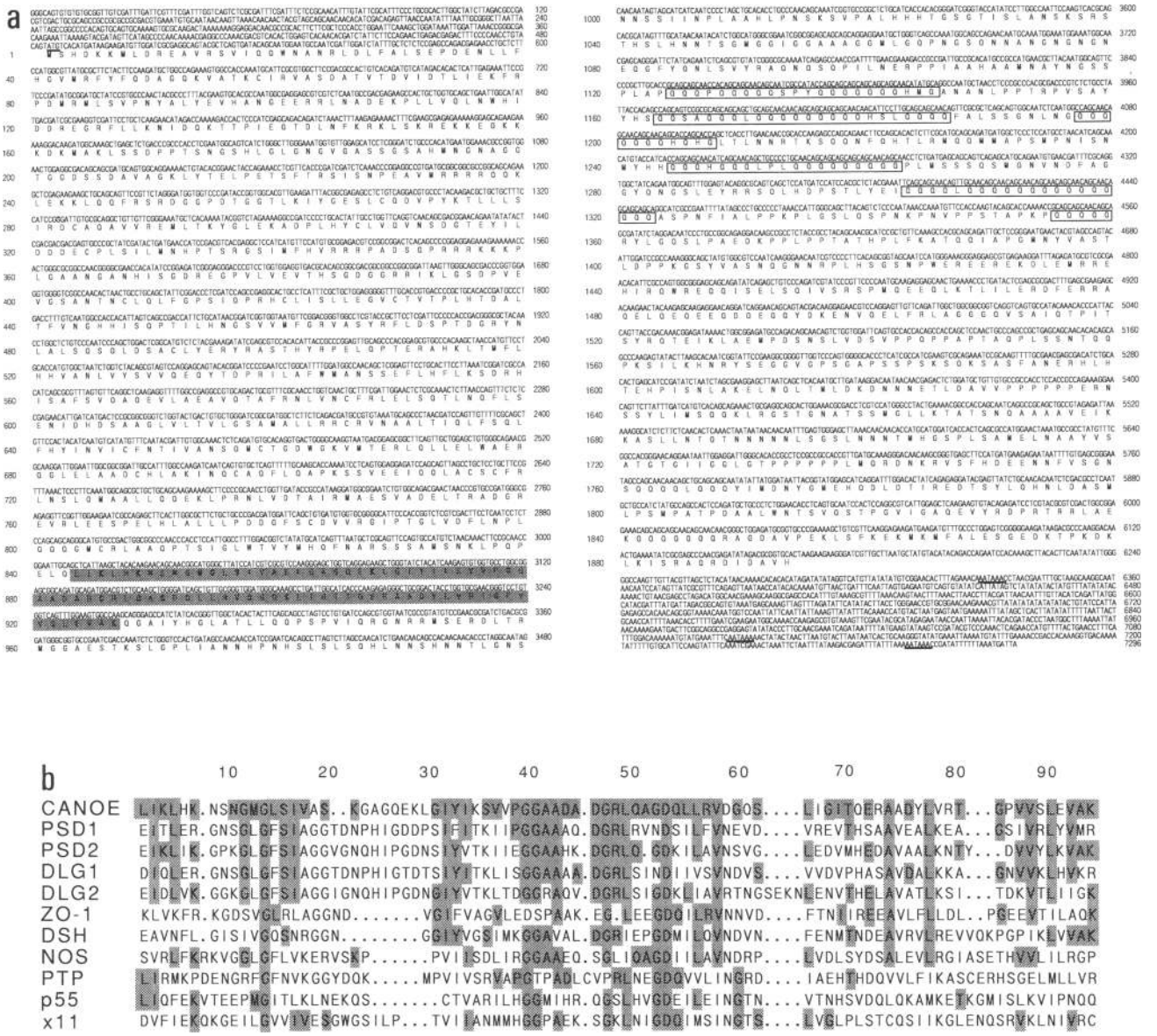

Figure 9. (*a*) The nucleotide and predicted protein sequences of *cno* cDNA. Underlined sequences include a potential translation initiation codon and putative polyadenylation signals. The *opa* repeat is boxed; the GLGF/DHR repeat is shaded. The sequence of the *cno* consensus cDNA was determined from five cDNAs. (*b*) Alignment of conserved amino acid sequences in the GLGF/DHR motif. Cno is compared with Dlg, Dsh, PSD95, NOS, ZO-1, p55, PTP-mag, and X11 (see text for abbreviations and references).

to differential poly adenylation. Unfortunately, the antiserum does not stain the tissue, so we were unable to determine Cno protein localization.

Discussion

In this study we have shown that mutations in the *cno* locus lead to fusions of ommatidia and duplications of bristles, just as *sca* and *N* mutations do. Beyond the phenotypic similarity among *cno*, *sca*, and *N*, we have demonstrated that these mutations genetically interact with each other during eye, bristle, and wing development. These observations suggest that *cno* has a common role with *sca* and *N* in the morphogenesis of diverse sets of tissues. The *sca* gene encodes a fibrinogen-like secreted protein with an EGF motif (Baker et al. 1990; Mlodzik et al. 1990). Genetic interactions between *sca* and *N* alleles in the developing compound eye have been reported by Baker et al. (1990), proposing that N is the receptor for Sca. On the other hand, Sca has been postulated to interact with or modify the extracellular matrix in a model proposed recently by Ellis et al. (1994), who found that constitutive activation of Sca^+ in the morphogenetic furrow in the developing eye disc results in improper spacing of facets, with the phenotype practically identical to the *sca* loss-of-function mutants. Their explana-

Downloaded from genesdev.cshlp.org on August 4, 2022 - Published by Cold Spring Harbor Laboratory Press

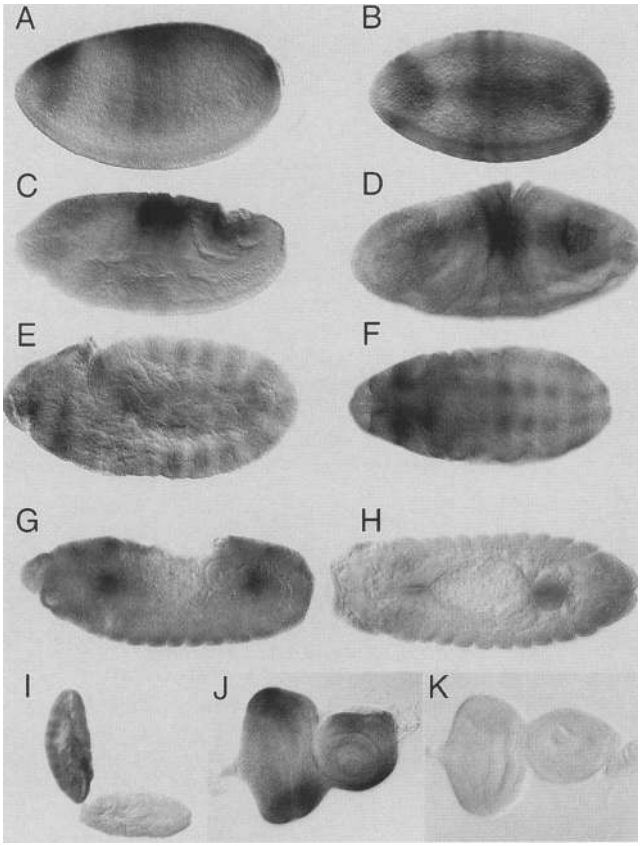

Figure 10. The expression pattern of *cno* mRNA revealed by in situ hybridization with the digoxygenin labeled antisense RNA probe. (*A–I*) Embryonic *cno* expression; (*J,K*) developing eye discs hybridized with antisense (*J*) or sense (*K*) probes of *cno* mRNA. Lateral (*A,C,E,G*) and dorsal (*B,D,F,H*) views of stage 5 (*A,B*), stage 7 (*C,D*), stage 10 (*E,F*), and stage 13 (*G,H*) wild-type embryos. Approximately one-fourth of the embryos of the *cno^{mis10}* balanced stock subjected to in situ hybridization with the antisense probe do not express *cno* mRNA at a detectable level (*I*). Stained and unstained stage 10 embryos from the *cno^{mis10}* stock are illustrated in *I*. In the eye disc, *cno* mRNA is present ubiquitously, with a higher level of expression in the lateral edge region (*J* vs. *K*).

tion is that Sca, as a protein having a homology with tenascin at its carboxyl terminus, participates in altering the cellular environment within clusters of neurogenic cells, protecting them from interference by inappropriate inductive signals (Ellis et al. 1994).

An important observation in this study is that the interrupted wing vein in *Ax^{1}*, a *N* allele producing an activated form of N protein (Rebay et al. 1993), is dominantly suppressed by *cno^{mis1}*. This indicates that *cno* is epistatic to *N*. Further support for the involvement of *cno* in the N pathway comes from the observation that extra wing veins are formed in *cno^{mis1}* homozygotes by reducing the gene dosage of *sgg^{+}*, a likely downstream component of *N* in the bristle development (Ruel et al. 1993). *sgg* also plays a role in producing cell fate diversity along the anterior–posterior axis in the embryo (Perrimon and Smouse 1989), presumably through its action on Armadillo (Arm), the *Drosophila* homolog of vertebrate β-catenin (Peifer et al. 1994; Noordermeer et al. 1994; Siegfried et al. 1994). Our preliminary observation that *cno^{mis1}* homozygotes become lethal when they are heterozygous for *arm^{YD35}* suggests a possible link between the *cno* and *arm* gene products in the signaling cascade.

Another adhesion molecule implicated to interact with the *cno* product is the β-subunit of the position-specific integrin (βPS) coded by the *mys* gene (Brown 1994). The *cno^{mis1}* mutation reduces viability of *mys^{NJ42}*, a hypomorphic allele of *mys* (Grinblat et al. 1994), and heterozygosity for the null allele, *mys^{XG43}*, promotes extra wing vein formation in *cno^{mis1}* homozygotes. It is intriguing that the genes encoding proteins involved in adhesive cell–cell communications, such as *arm* (β-catenin), *mys* (βPS integrin), and *N* itself (Cagan and Ready 1989), are shown to interact with *cno*. A reduction in the gene dosage of *arm*, *mys*, or *N* results in obvious enhancement of the *cno^{mis1}* phenotypes, suggesting that the genetic interactions among these genes are specific. The Arm (Peifer 1993), Mys (Brown 1994), and N (Fehon et al. 1991) proteins are tightly localized to the adherens junctions, the most apical junctional complex where elements of the cytoskeleton are closely associated with the cell membrane (Tepass and Hartenstein 1993). These proteins could mediate the adhesion of the different cell layers in a variety of developing tissues. In the developing adult wing, for example, Mys (Wilcox et al. 1981) and N (Kidd et al. 1989) are expressed in both the presumptive dorsal and ventral cells. During metamorphosis, the basal surface of the dorsal cell layer becomes attached to the basal surface of the ventral cell layer and the two surfaces are connected by large adherens junctions (Fristrom et al. 1993). In mosaic clones of *mys* mutant cells within the adult wing, the two surfaces of the wing blade separate (Brower and Jaffe 1989; Zusman et al. 1990). The crumpled appearance of the wings of *cno^{mis1}/Df(3R)6-7, spl*; *cno^{mis1}, sca^{1}*; *cno^{mis1}*, and *N^{55e11}/+*; *cno^{mis1}* flies may result from incomplete adhesion of the dorsal and ventral cell layers.

In concert with the results of phenotypic analysis, molecular characterization of *cno* provides circumstantial evidence to support the notion that the *cno* product mediates adhesive interactions between cells. The sequence of *cno* suggests an intracellular protein that shares an amino acid motif (GLGF/DHR repeat) with several proteins that are localized to cell junctions (i.e., Dlg, PSD-95, and ZO-1) or to junction-like complexes (p55) (Woods and Bryant 1993). It is conceivable that Cno is localized to junctional complexes, although we have not demonstrated this experimentally, as our anti-Cno antibody was not a useful probe for immunohistochemistry.

The Dsh protein of *Drosophila* has the GLGF/DHR repeat (Klingensmith et al. 1994; Theisen et al. 1994). A hypothesis has been proposed that *dsh* function in embryogenesis transduces the *wingless* (*wg*) signal and eventually alters the intracellular distribution of Arm, which is otherwise associated with the adherens junc-

Downloaded from genesdev.cshlp.org on August 4, 2022 - Published by Cold Spring Harbor Laboratory Press

tion (Noordermeer et al. 1994). Recently, it was suggested that Dsh may bind directly to N (Axelrod and Perrimon 1994). The importance of this finding is twofold. First, it raises the possibility that proteins with the GLGF/DHR repeat (e.g., Dsh and Cno) may mediate cross talk between different transduction cascades (e.g., the N pathway and the Wg pathway; Hing et al. 1994). Second, it proves that N is a multiligand receptor that can activate distinct downstream signaling mechanisms depending on the developmental context. From these considerations, we hypothesize that Cno is a cytoplasmic protein associated with N, mediating the interactions of the N cascade with other signaling pathways. It remains to be determined whether the association of Cno with N is direct or indirect. This issue may be addressed by examining whether the anti-Cno antibody is capable of coprecipitating the N protein. Another approach would be to use the yeast two-hybrid system, which was designed to detect protein–protein interactions as a result of their ability to reconstitute the *trans*-activating function of the GAL4 protein (Zervos et al. 1993). With this technique, the *deltex* product was shown to bind with the ankyrin repeats to the cytoplasmic domain of N (Diederich et al. 1994). Does Cno bind to N? If so, what would be a role for the GLGF/DHR repeat in this association? These are clearly the most significant questions to be answered in elucidating the molecular mechanism of the Cno functions in *Drosophila* development.

Materials and methods

Mutagenesis

Mutagenesis was initiated by crossing two strains, one of which contained a jump starter element encoding P-element transposase, which efficiently mobilizes the second nonautonomous transposon (mutator), whose structure facilitates the selection of new insertion mutations and cloning of mutated genes (Cooley et al. 1988). The Δ2-3 strain (Robertson et al. 1988) was used as a jump starter, whereas a strain carrying the BmΔw transposon (Steller and Pirrotta 1985) was used as a mutator. All flies used had w^- background, whereas the BmΔw carried a copy of modified w^+, allowing us to recover chromosomes with BmΔw insertions by selecting individuals with non-white eye color.

The resulting fly stocks with P-element insertions were examined for roughness of the eyes, which led to isolation of mis^1. By introducing the Δ2-3 chromosome to the mis^1 line, the mutator element was remobilized, resulting in many lines with white eyes. mis^{10} and mis^{r13} were representative of these lines. All *mis* chromosomes were maintained in *trans* with the TM3 balancer.

Chromosome in situ hybridizations

We employed the plasmid rescue method (Hanahan et al. 1980) using the plasmid sequences included in the P element to recover DNA sequences flanking the P-element insertion point. The rescued plasmid from the mis^1 line was labeled with bio-11dUTP (Enzo Biochemicals) by nick translation. Polytene chromosomes were prepared from salivary glands of late third instar larvae of the *w* strain. Signal detection was performed with streptavidin-conjugated alkali phosphatase (BRL) followed by histochemical detection with nitroblue tetrazolium and BCIP.

Somatic recombination technique and mosaic analysis

Heterozygotes for mosaic analysis using *w* markers were generated by crossing *w*; P925 to *w*; mis^{10}/*TM3*. X-irradiation (1200 rads) of the progeny was carried out between 0 and 48 hr of development (Tei et al. 1992). Mosaic eyes were identified as white patches in otherwise pigmented eyes. The frequency of generating mosaic eyes was 1/500. Morphologically, wild-type mosaic ommatidia from 11 individuals were examined. Mosaic eyes were fixed and embedded, and serial 1.5-μm sections were obtained along the long axis of the eye. Individual ommatidia were identified and followed from distal (~10 μm in depth from the surface of the eye) to proximal (~90 μm from the surface) in ~15-μm steps to avoid error in scoring the absence or presence of pigments.

Histology

Tissue was fixed for 15 min in a chilled mixture of 1% glutaraldehyde and 1% osmium tetroxide in 0.1 M phosphate buffer. After a buffer wash, tissue was postfixed in chilled 2% osmium tetroxide in phosphate buffer for 1 hr and dehydrated through a graded alcohol series. After absolute alcohol, the tissue was transferred to propylene oxide to which an equal volume of Epon was added. This mixture was left overnight and then replaced with pure Epon for 4 hr. The tissue was then embedded in Epon and polymerized. For light microscopy, semithin sections (1.0 μm) were stained with methylene blue or toluidine blue. For scanning electron microscopy, the flies were prepared by critical point drying and coated with 2 nm of gold. Images were taken on a low-voltage prototype SEM. Eye discs from late third instar larvae were dissected out and stained for β-galactosidase activity or with mAb 22C10 as described in Krämer et al. (1991). Cobalt sulfide stainings of pupal eye discs were carried out according to the method described in Cagan and Ready (1989).

DNA isolation and sequencing

The plasmid rescue method was used to recover a genomic DNA fragment flanking the P-element insertion point. The rescued DNA fragment was used to initiate a genomic walk using a λ EMBL3 Canton-S genomic library (Clontech Laboratories, Inc.). Genomic clones that cover exons 5–15 were obtained by screening the library with a probe composed of the 3 'end of a cDNA (see below). A 5-kb *Eco*RI fragment in the rescued genomic DNA was used to screen an eye imaginal disc cDNA library (constructed by A. Cowman). One positive phage containing a 0.3-kb insert was obtained. Subsequently the 0.3-kb cDNA fragment was used as a probe to screen a λgt11 embryonic cDNA library (Zinn et al. 1988). Through four successive rounds of library screening, four overlapping cDNA clones were isolated. Genomic DNAs and cDNAs were subcloned into the pBluescript (Stratagene) or pUC19 vector and restriction mapped. Sequencing of genomic DNA and cDNA clones was performed by the chain termination method (Sanger et al. 1977) using Sequenase (U.S. Biochemical).

Northern blot analysis

Total RNA was isolated by the single-step method (Chomczynski and Sacchi 1987), and poly(A)$^+$ RNA was prepared by oli-

Downloaded from genesdev.cshlp.org on August 4, 2022 - Published by Cold Spring Harbor Laboratory Press

go(dT)–cellulose affinity chromatography using an mRNA purification kit (Pharmacia LKB). Five micrograms of poly(A)$^+$ RNA was separated on 1% agarose gel containing formaldehyde as described (Sambrook et al. 1989). Following transfer to Nitroplus 2000 (Micron Separations Inc.), the filter was hybridized in 6× SSC, 5× Denhardt's solution, 0.5% SDS, 4 mM EDTA, 100 μg/ml of salmon sperm DNA, and ^{32}P-labeled probes (>10^8 cpm/μg) at 65°C. The filter was washed in 0.5× SSC at 60°C and then exposed to x-ray film.

Primer extension analysis

Poly(A)$^+$ RNA from 0- to 12-hr embryos (5 μg) was hybridized with ^{32}P-labeled oligonucleotide primer (10^5 cpm) complementary to nucleotides 46–70 of *cno* cDNA (Fig. 9a). The primer was extended with Moloney murine leukemia virus (Mo-MLV) reverse transcriptase at 37°C for 1 hr, and the reaction product was electrophoresed on an 8 M urea/6% polyacrylamide gel.

Preparation of antiserum

A nucleotide sequence corresponding to amino acid residues 122–258 was amplified by the polymerase chain reaction and ligated into the pGEX-3X vector (Smith and Johnson 1988). The plasmid was introduced into XL-1 blue cells, and a fusion protein with GST was induced by IPTG. After 5 hr of culture, cells were pelleted and resuspended in 50 mM Tris (pH 7.5), 25% sucrose, 0.5% NP-40, 5 mM $MgCl_2$, and 100 μM (*p*-amidinophenyl) methanesulfonyl fluoride (p-APMSF). Cells were lysed by sonication for 5 min and centrifuged. The supernatant was mixed with glutathione–agarose beads (Sigma) at 4°C for 30 min. The fusion protein was eluted with 5 mM glutathione and analyzed on a SDS–10% polyacrylamide gel (Laemmli 1970). A rabbit antiserum was raised against the fusion protein. After three cycles of immunization the antiserum was collected and applied to a GST affinity column. The flowthrough fraction was purified further by fusion protein affinity chromatography.

Western blot analysis

Embryos of Canton-S (0- to 12 hr) were homogenized in 1× Laemmli sample buffer containing p-APMSF. After boiling for 5 min, the lysates were centrifuged at 10,000 rpm for 5 min. Protein concentrations of the supernatants were determined by the dye-binding method (Bradford 1976). Samples containing 100 μg of protein were electrophoresed on a SDS–5% polyacrylamide gel and transfered to Immobilon PVDF membrane (Millipore Corporation) as described (Towbin et al. 1979). The blot was incubated with antiserum, followed by incubation with horseradish peroxidase-conjugated goat anti-rabbit IgG (Bio-Rad). Immunologically reactive proteins were visualized in 1 mg/ml of 3,3′-diaminobenzidine tetrahydrochloride, 0.02% H_2O_2, and 0.4 mg/ml of $NiCl_2$.

Tissue in situ hybridization

In situ hybridization to whole-mount discs was performed according to the protocol of Tautz and Pfeifle (1989). The imaginal discs were dissected in PBS and fixed in 4% paraformaldehyde and 0.5% Triton X-100 in PBS for 15–20 min. All incubations and washes were performed at room temperature. After three 5-min washes in PBS/0.1% Tween, the discs were digested with proteinase K (12.5 μg/ml in PBS/0.1% Tween) for 4–10 min. Following digestion, the discs were washed once in PBS/0.1% Tween and 2 mg/ml of glycine for 10 min and twice for 5 min each in PBS/0.1% Tween, before being fixed for 20 min with 4% paraformaldehyde and 0.2% glutaraldehyde in PBS. Following four 5-min washes in PBS/0.1% Tween, the discs were prehybridized and hybridized as described by Tautz and Pfeifle (1989). Nonradioactive probes were made by using digoxigenin–UTP and detected with monoclonal antibody against digoxigenin coupled to alkaline phosphatase according to the manufacturer's instructions (Boehringer Mannheim). Essentially, the same protocol was used for in situ hybridization to whole-mount embryos.

Acknowledgments

We thank Steven Wasserman, Christiane Nüsslein-Volhard, Petter Portin, Pat Simpson, Richard O. Hynes, Eric Wieschaus, Larry Zipursky, the Bowling Green Stock Center and the Bloomington Stock Center for fly stocks, and Gerry Rubin and Kai Zinn for cDNA libraries. We are grateful to J. Larry Marsh and members of the Yamamoto laboratory for their comments on drafts of this manuscript. We also thank Kei Ito for technical guidance in cobalt sulfide staining, Kazue Usui for preparing some fly lines, and Yasuko Matsumura for secretarial assistance. This work was supported by grants from Mitsubishi Kasei Institute of Life Sciences, The Brain Science Fundation, and the Ministry of Education, Science and Culture of Japan (05263102).

The publication costs of this article were defrayed in part by payment of page charges. This article must therefore be hereby marked "advertisement" in accordance with 18 USC section 1734 solely to indicate this fact.

References

Artavanis-Tsakonas, S., C. Delidakis, and R.G. Fehon. 1991. The *Notch* locus and the cell biology of neuroblast segregation. *Annu. Rev. Cell Biol.* **7:** 427–452.

Axelrod, J. and N. Perrimon. 1994. "*dishevelled* mediates *wingless* and *Notch* signaling in determining cell fates on the *Drosophila* wing margin." Thirty-fifth Annual *Drosophila* Research Conference Program and Abstracts Volume, 35B.

Baker, N.E., M. Mlodzik, and G.M. Rubin. 1990. Spacing differentiation in the developing *Drosophila* eye: A fibrinogen-related lateral inhibitor encoded by *scabrous*. *Science* **250:** 1370–1377.

Baker, N.E., K. Moses, D. Nakahara, M.C. Ellis, R.W. Carthew, and G.M. Rubin. 1992. Mutations on the second chromosome affecting the *Drosophila* eye. *J. Neurogenet.* **8:** 85–100.

Bang, A.G., V. Hartenstein, and J.W. Posakony. 1991. *Hairless* is required for the development of adult sensory organ precursor cells in *Drosophila*. *Development* **111:** 89–104.

Basler, K. and E. Hafen. 1991. Specification of cell fate in the developing eye of *Drosophila*. *BioEssays* **13:** 621–631.

Bradford, M.M. 1976. A rapid and sensitive method for the quantitation of microgram quantities of protein utilizing the principle of protein-dye binding. *Ann. Biochem.* **72:** 248–254.

Bredt, D.S., P.M. Hwang, C.E. Glatt, C. Lowenstein, R.R. Read, and S.H. Snyder. 1991. Cloned and expressed nitric oxide synthase structurally resembles cytochrome P-450 reductase. *Nature* **351:** 714–718.

Brower, D.L. and S.M. Jaffe. 1989. Requirement for integrins during *Drosophila* wing development. *Nature* **342:** 285–287.

Brown, N.H. 1994. Null mutations in the αps2 and βps integrin subunit genes have distinct phenotypes. *Development* **120:** 1221–1231.

Cagan, R.L. and D.F. Ready. 1989. Notch is required for succes-

Downloaded from genesdev.cshlp.org on August 4, 2022 - Published by Cold Spring Harbor Laboratory Press

sive cell decisions in the developing *Drosophila* retina. *Genes & Dev.* **3:** 1099–1112.

Campos-Ortega, J.A. 1993. Mechanisms of early neurogenesis in *Drosophila melanogaster. J. Neurobiol.* **24:** 1305–1327.

Cho, K.-O., C.A. Hunt, and M.B. Kennedy. 1992. The rat brain postsynaptic density fraction contains a homolog of the Drosophila discs-large tumor suppressor protein. *Neuron* **9:** 929–942.

Chomczynski, P. and N. Sacchi. 1987. Single-step method of RNA isolation by acid guanidinium thiocyanate–phenol–chloroform extraction. *Ann. Biochem.* **162:** 156–159.

Cooley, L., R. Kelly, and A. Spradling. 1988. Insertional mutagenesis of the *Drosophila* genome with single P elements. *Science* **239:** 1121–1128.

Coyle-Thompson, C.A. and U. Banerjee. 1993. The *strawberry notch* gene functions with *Notch* in common developmental pathways. *Development* **119:** 377–395.

de Celis, J.F. and A. García-Bellido. 1994. Roles of the *Notch* gene in *Drosophila* wing morphogenesis. *Mech. Dev.* **46:** 109–122.

Diederich, R.J., K. Matsuno, H. Hing, and S. Artavanis-Tsakonas. 1994. Cytosolic interaction between deltex and Notch ankyrin repeats implicates deltex in the Notch signaling pathway. *Development* **120:** 473–481.

Duclos, F., U. Boschert, G. Sirugo, J.L. Mandel, R. Hen, and M. Koenig. 1993. Gene in the region of the Friedreich ataxia locus encodes a putative transmembrane protein expressed in the nervous system. *Proc. Natl. Acad. Sci.* **90:** 109–113.

Ellis, M.C., U. Weber, V. Wiersdorff, and M. Mlodzik. 1994. Confrontation of *scabrous* expressing and non-expressing cells is essential for normal ommatidial spacing in the *Drosophila* eye. *Development* **120:** 1959–1969.

Fehon, R.G., K. Johansen, I. Rebay, and S. Artavanis-Tsakonas. 1991. Complex spacial and temporal regulation of *Notch* expression during embryonic and imaginal development of *Drosophila*: Implications for *Notch* function. *J. Cell Biol.* **113:** 657–669.

Fortini, M.E., I. Rebay, L.A. Caron, and S. Artavanis-Tsakonas. 1993. An activated Notch receptor blocks cell-fate commitment in the developing *Drosophila* eye. *Nature* **365:** 555–557.

Fristrom, D., M. Wilcox, and J. Fristrom. 1993. The distribution of PS integrins, laminin A and F-actin during key stages in *Drosophila* wing development. *Development* **117:** 509–523.

Grinblat, Y., S. Zusman, G. Yee, R.O. Hynes, and F.C. Kafatos. 1994. Functions of the cytoplasmic domain of the βps integrin submit during *Drosophila* development. *Development* **120:** 91–102.

Gu, M.X., J.D. York, I. Warshawsky, and P.W. Majerus. 1991. Identification, cloning, and expression of a cytosolic megakaryocyte protein-tyrosine-phosphatase with sequence homology to cytoskeletal protein 4.1. *Proc. Natl. Acad. Sci.* **88:** 5867–5871.

Hanahan, D., D. Lane, L. Lipsich, M. Wigler, and M. Botchan. 1980. Characteristics of an SV-40 plasmid recombinant and its movement into and out of the genome of a murine cell. *Cell* **21:** 127–139.

Hartenstein, A.Y., A. Rugendorff, U. Tepass, and V. Hartenstein. 1992. The function of the neurogenic genes during epithelial development in the *Drosophila* embryo. *Development* **116:** 1203–1220.

Hetzler, P. and P. Simpson. 1991. The choice of cell fate in the epidermis of *Drosophila. Cell* **64:** 1083–1092.

Hing, H.-K., X. Sun, and S. Artavanis-Tsakonas. 1994. Modulation of wingless signaling by Notch in *Drosophila. Mech. Dev.* **47:** 261–268.

Itoh, M., A. Nagafuchi, S. Yonemura, T. Kitani-Yasuda, S. Tsukita, and S. Tsukita, 1993. The 220-kD protein colocalizing with cadherins in non-epithelial cells is identical to ZO-1, a tight junction-associated protein in epithelial cells: cDNA cloning and immunoelectron microscopy. *J. Cell Biol.* **121:** 491–502.

Jürgens, G., E. Wieschaus, C. Nüsslein-Volhard, and H. Kluding. 1984. Mutations affecting the pattern of the larval cuticle in *Drosophila melanogaster. Wilhelm Roux's Arch. Dev. Biol.* **193:** 283–295.

Kidd, S., M.R. Kelley, and M.W. Young. 1986. Sequence of the Notch locus of *Drosophila melanogaster*: Relationship of the encoded protein to mammalian clotting and growth factors. *Mol. Cell. Biol.* **6:** 3094–3108.

Kidd, S., M.K. Baylier, G.P. Gasic, and M.W. Young. 1989. Structure and distribution of the Notch protein in developing *Drosophila. Genes & Dev.* **3:** 1113–1129.

Klingensmith, J., R. Nusse, and N. Perrimon. 1994. The *Drosophila* segment polarity gene *dishevelled* encodes a novel protein required for response to the *wingless* signal. *Genes & Dev.* **8:** 118–130.

Krämer, H., R.L. Cagan, and S.L. Zipursky. 1991. Interaction of Bride of sevenless membrane-bound ligand and the Sevenless tyrosine-kinase receptor. *Nature* **352:** 207–212.

Laemmli, U.K.. 1970. Cleavage of structural proteins during the assembly of the head of bacteriophage T4. *Nature* **227:** 680–685.

Leptin, M., T. Bogaert, R. Lehmann, and M. Wilcox. 1989. The function of PS integrins during Drosophila embryogenesis. *Cell* **56:** 401–408.

Lieber, T., S. Kidd, E. Alcamo, V. Corbin, and M.W. Young. 1993. Antineurogenic phenotypes induced by truncated Notch proteins indicate a role in signal transduction and may point to a novel function for Notch in nuclei. *Genes & Dev.* **7:** 1949–1965.

Mlodzik, M., N.E. Baker, and G.M. Rubin. 1990. Isolation and expression of *scabrous*, a gene regulating neurogenesis in *Drosophila. Genes & Dev.* **4:** 1848–1861.

Noordermeer, J., J. Klingensmith, N. Perrimon, and R. Nusse. 1994. *dishevelled* and *armadillo* act in the *wingless* signalling pathway in *Drosophila. Nature* **367:** 80–83.

Peifer, M. 1993. The product of the *Drosophila* segment polarity gene *armadillo* is part of a multi-protein complex resembling the vertebrate adherens junction. *J. Cell Sci.* **105:** 993–1000.

Peifer, M., D. Sweeton, M. Casey, and E. Wieschaus. 1994. *wingless* signal and *zeste-white 3* kinase trigger opposing changes in the intracellular distribution of Armadillo. *Development* **120:** 369–380.

Perrimon, N. and D. Smouse. 1989. Multiple functions of a *Drosophila* homeotic gene, *zeste-white 3*, during segmentation and neurogenesis. *Dev. Biol.* **135:** 287–305.

Ready, D.F. 1989. A multifaceted approach to neural development. *Trends Neurosci.* **12:** 102–110.

Rebay, I., R.J. Fleming, R.G. Fehon, L. Cherbas, P. Cherbas, and S. Artavanis-Tsakonas. 1991. Specific EGF repeats of Notch mediate interactions with Delta and Serrate: Implications for Notch as a mulifunctional receptor. *Cell* **67:** 687–699.

Rebay, I., R.G. Fehon, and S. Artavanis-Tsakonas. 1993. Specific truncations of Drosophila Notch define dominant activated and dominant negative forms of the receptor. *Cell* **74:** 319–329.

Renfranz, P.J. and S. Benzer. 1989. Monoclonal antibody probes discriminate early and late mutant defects in development of the *Drosophila* retina. *Dev. Biol.* **136:** 411–429.

Reuter, R., B. Grunewald, and M. Leptin. 1993. A role for the

Downloaded from genesdev.cshlp.org on August 4, 2022 - Published by Cold Spring Harbor Laboratory Press

mesoderm in endodermal migration and morphogenesis in *Drosophila*. *Development* **119:** 1135–1145.

Robertson, H.M., C.R. Preston, R.W. Phillis, D.M. Johnson-Schlitz, W.K. Denz, and W.R. Engels. 1988. A stable sourse of P-element transposase in *Drosophila melanogaster*. *Genetics* **118:** 461–470.

Rubin, G.M. 1988. *Drosophila melanogaster* as an experimental organism. *Science* **240:** 1453–1459.

Ruel, L., M. Bourouis, P. Heitzler, V. Pantesco, and P. Simpson. 1993. *Drosophila shaggy* kinase and rat glycogen synthase kinase-3 have conserved activities and act downstream of *Notch*. *Nature* **362:** 557–560.

Ruff, P., D.W. Speicher, and A. Husain-Chishti. 1991. Molecular identification of a major palmitoylated erythrocyte membrane protein containing the src homology 3 motif. *Proc. Natl. Acad. Sci.* **88:** 6595–6599.

Ruohola, H., K.A. Bremer, D. Baker, J.R. Swedlow, L.Y. Jan, and Y.N. Jan. 1991. Role of neurogenic genes in establishment of follicle cell fate and oocyte polarity during oogenesis in Drosophila. *Cell* **66:** 433–449.

Sambrook, J., E.F. Fritsch, and T. Maniatis. 1989. *Molecular cloning: A laboratory manual*, 2nd ed. Cold Spring Harbor Laboratory Press, Cold Spring Harbor, New York.

Sanger, F., S. Nichlen, and A.R. Coulson. 1977. DNA sequencing with chain-terminating inhibitors. *Proc. Natl. Acad. Sci.* **74:** 5463–5467.

Siegfried, E., E.L. Wilder, and N. Perrimon. 1994. Components of *wingless* signalling in Drosophila. *Nature* **367:** 76–79.

Smith, D.B. and K.S. Johnson. 1988. Single step purification of polypeptides expressed in Escherichia coli as fusions with glutathione S-transferase. *Gene* **67:** 31–40.

Steller, H. and V. Pirrotta. 1985. A transposable P vector that confers selectable G418 resistance to Drosophila larvae. *EMBO J.* **4:** 167–171.

Tautz, D. and C. Pfeifle. 1989. A non-radioactive in situ hybridization method for the localization of specific RNAs in *Drosophila* embryos reveals translational control of the segmentation gene *hunchback*. *Chromosoma* **98:** 81–85.

Tei, H., I. Nihonmatsu, T. Yokokura, R. Ueda, Y. Sano, T. Okuda, K. Sato, K. Hirata, S.C. Fujita, and D. Yamamoto. 1992. *pokkuri*, a *Drosophila* gene encoding an E-26-specific (Ets) domain protein, prevents overproduction of the R7 photoreceptor. *Proc. Natl. Acad. Sci.* **89:** 6856–6860.

Tepass, U. and V. Hartenstein. 1993. The development of cellular junctions in the *Drosophila* embryo. *Dev. Biol.* **161:** 563–596.

———. 1994. Epithelium formation in the *Drosophila* midgut depends on the interaction of endoderm and mesoderm. *Development* **120:** 579–590.

Theisen, H., J. Purcell, M. Bennett, D. Kansagara, A. Syed, and J.L. Marsh. 1994. *dishevelled* is required during *wingless* signaling to establish both cell polarity and cell identity. *Development* **120:** 347–360.

Tomlinson, A. 1988. Cellular interactions in the developing *Drosophila* eye. *Development* **104:** 183–193.

Towbin, H.T., T. Staehelin, and J. Gordon. 1979. Electrophoretic transfer of protein from polyacrylamide gels to nitrocellulose sheets: procedure and some applications. *Proc. Natl. Acad. Sci.* **76:** 4350–4354.

Wharton, K.A., K.M. Johansen, T. Xu, and S. Artavanis-Tsakonas. 1985. Nucleotide sequence from the neurogenic locus Notch implies a gene product that shares homology with proteins containing EGF-like repeats. *Cell* **43:** 567–581.

Wilcox, M., D.L. Brower, and R.J. Smith. 1981. A position-specific cell surface antigen in the Drosophila wing imaginal disc. *Cell* **25:** 159–164.

Woods, D.F. and P.J. Bryant. 1991. The *discs-large* tumor suppressor gene of Drosophila encodes a guanylate kinase homolog localized at septate junctions. *Cell* **66:** 451–464.

———. 1993. ZO1, DlgA and PSD-95/SAP90: Homologous proteins in tight, septate and synaptic cell junctions. *Mech. Dev.* **44:** 85–89.

Xu, T., I. Rebay, R.J. Fleming, T.N. Scottgale, and S. Artavanis-Tsakonas. 1990. The *Notch* locus and the genetic circuitry involved in early *Drosophila* neurogenisis. *Genes & Dev.* **4:** 464–475.

Yamamoto, D. 1993. Positive and negative signaling mechanisms in the regulation of photoreceptor induction in the developing *Drosophila* retina. *Genetica* **88:** 153–164.

———. 1994. Signaling mechanisms in induction of the R7 photoreceptor in the developing *Drosophila* retina. *BioEssays* **16:** 237–244.

Zervos, A.S., J. Gyuris, and R. Brent. 1993. Mxil, a protein that specifically interacts with Max to bind Myo-Max recognition sites. *Cell* **72:** 223–232.

Zinn, K., L. McAllister, and C.S. Goodman. 1988. Sequence analysis and neuronal expression of fasciclin I in grasshopper and Drosophila. *Cell* **53:** 577–587.

Zipursky, S.L. 1989. Molecular and genetic analysis of *Drosophila* eye development. *sevenless, bride of sevenless* and *rough*. *Trends Neurosci.* **12:** 183–189.

Zusman, S., R.S. Patel-King, C. ffrench-Constant, and R.O. Hynes. 1990. Requirements for integrin functions during *Drosophila* development. *Development* **118:** 737–750.

Downloaded from genesdev.cshlp.org on August 4, 2022 - Published by Cold Spring Harbor Laboratory Press

canoe encodes a novel protein containing a GLGF/DHR motif and functions with Notch and scabrous in common developmental pathways in Drosophila.

H Miyamoto, I Nihonmatsu, S Kondo, et al.

Genes Dev. 1995, **9:**
Access the most recent version at doi:10.1101/gad.9.5.612

References This article cites 74 articles, 32 of which can be accessed free at:
http://genesdev.cshlp.org/content/9/5/612.full.html#ref-list-1

License

Email Alerting Service Receive free email alerts when new articles cite this article - sign up in the box at the top right corner of the article or **click here.**

Copyright © Cold Spring Harbor Laboratory Press